Methylated DNA Causes a Physical Block to Replication Forks Independently of Damage Signalling, O6-Methylguanine or DNA Single-Strand Breaks and Results in DNA Damage

Groth, P; Ausländer, S; Majumder, MM; Schultz, N; Johansson, F; Petermann, Eva; Helleday, T

DOI:
10.1016/j.jmb.2010.07.010

Document Version
Publisher final version (usually the publisher pdf)

Citation for published version (Harvard):
Groth, P, Ausländer, S, Majumder, MM, Schultz, N, Johansson, F, Petermann, E & Helleday, T 2010, 'Methylated DNA Causes a Physical Block to Replication Forks Independently of Damage Signalling, O6-Methylguanine or DNA Single-Strand Breaks and Results in DNA Damage' Journal of Molecular Biology, vol 402, no. 1, pp. 70-82., 10.1016/j.jmb.2010.07.010

doi:10.1016/j.jmb.2010.07.010 J. Mol. Biol. (2010) 402, 70–82

JMB

Available online at www.sciencedirect.com

ScienceDirect

ELSEVIER

Methylated DNA Causes a Physical Block to Replication Forks Independently of Damage Signalling, O^6-Methylguanine or DNA Single-Strand Breaks and Results in DNA Damage

Petra Groth[1], Simon Ausländer[1], Muntasir Mamun Majumder[1], Niklas Schultz[1], Fredrik Johansson[1], Eva Petermann[2] and Thomas Helleday[1,2]*

[1]*Department of Genetics, Microbiology and Toxicology, Stockholm University, S-106 91 Stockholm, Sweden*

[2]*Gray Institute for Radiation Oncology and Biology, University of Oxford, Old Road Campus Research Building, Off Roosevelt Drive, Oxford OX3 7DQ, UK*

Received 12 April 2010; received in revised form 1 July 2010; accepted 12 July 2010
Available online 17 July 2010

Even though DNA alkylating agents have been used for many decades in the treatment of cancer, it remains unclear what happens when replication forks encounter alkylated DNA. Here, we used the DNA fibre assay to study the impact of alkylating agents on replication fork progression. We found that the alkylator methyl methanesulfonate (MMS) inhibits replication elongation in a manner that is dose dependent and related to the overall alkylation grade. Replication forks seem to be completely blocked as no nucleotide incorporation can be detected following 1 h of MMS treatment. A high dose of 5 mM caffeine, inhibiting most DNA damage signalling, decreases replication rates overall but does not reverse MMS-induced replication inhibition, showing that the replication block is independent of DNA damage signalling. Furthermore, the block of replication fork progression does not correlate with the level of DNA single-strand breaks. Overexpression of O^6-methylguanine (O6meG)-DNA methyltransferase protein, responsible for removing the most toxic alkylation, O6meG, did not affect replication elongation following exposure to *N*-methyl-*N*′-nitro-*N*-nitrosoguanidine. This demonstrates that O6meG lesions are efficiently bypassed in mammalian cells. In addition, we find that MMS-induced γH2AX foci co-localise with 53BP1 foci and newly replicated areas, suggesting that DNA double-strand breaks are formed at MMS-blocked replication forks. Altogether, our data suggest that N-alkylations formed during exposure to alkylating agents physically block replication fork elongation in mammalian cells, causing formation of replication-associated DNA lesions, likely double-strand breaks.

Keywords: *N*-methyl-*N*′-nitro-*N*-nitrosoguanidine; methyl methanesulfonate; mammalian cells; replication fork elongation; double-strand breaks

Edited by J. Karn

**Corresponding author*. Gray Institute for Radiation Oncology and Biology, University of Oxford, Old Road Campus Research Building, Off Roosevelt Drive, Oxford OX3 7DQ, UK. E-mail address: thomas.helleday@rob.ox.ac.uk.

Abbreviations used: MMS, methyl methanesulfonate; O6meG, O^6-methylguanine; MNNG, *N*-methyl-*N*′-nitro-*N*-nitrosoguanidine; N7meG, N^7-methylguanine; N3meA, N^3-methyladenine; BER, base excision repair; SSB, single-strand break; MGMT, O6meG-DNA methyltransferase; DSB, double-strand break; HR, homologous recombination; TLS, translesion synthesis; CldU, 5-chlorodeoxyuridine; IdU, 5-iododeoxyuridine; GFP, green fluorescent protein; FACS, fluorescence-activated cell sorting; PFGE, pulse-field gel electrophoresis; HBSS, Hanks balanced salt solution; PBS, phosphate-buffered saline; PBS-T, PBS containing 0.1% Triton X-100.

0022-2836/$ - see front matter

Introduction

Alkylating agents are widely used in the treatment of a range of cancers,[1] and for development of more specific treatments, it is important to outline the mechanism triggered by these agents. Alkylators are electrophilic compounds that are attracted to the nucleophilic centres of DNA bases, primary exocylic oxygen and nitrogen residues. The compounds attach alkyl groups reacting with S_N1 or S_N2 mechanism determining the ratio of oxygen to nitrogen modifications. The most commonly alkylated site is the N^7 position of guanine, which has the highest negative electrostatic potentials of the nucleophilic sites of DNA.[2] Methyl methanesulfonate (MMS) and *N*-methyl-*N*′-nitro-*N*-nitrosoguanidine (MNNG) are well used as model compounds for alkylators and produce DNA methyl adducts[3] but with different reaction mechanisms. For both compounds, the predominant lesions induced are N^7-methylguanine (N7meG) followed by N^3-methyladenine (N3meA).[4] The main difference between MMS and MNNG lies in the induction of O^6-methylguanine (O6meG), the major toxic and mutagenic lesion produced by methylating agents.[5,6] The proposed mechanism for these properties is mismatch-repair-mediated futile repair affecting the second round of replication.[7] Only 0.3% of total alkylations induced by S_N2 reacting compound MMS are O6meG compared to 7% produced by MNNG treatment,[3] and therefore, MNNG is more suitable for investigations of the effects of O6meG.

The base damage caused by alkylating agents is mainly repaired by base excision repair (BER), where alkylations such as N7meG and N3meA are repaired in a rapid multistep process. Glycosylases specific for the damage remove the damaged base leaving an apurinic site (AP site) as intermediate. Removal of the damaged base is followed by endonuclease cleavage of the AP site creating a single-strand break (SSB) and a DNA gap. The DNA gap will then be polymerised and ligated where both processes are stabilised by XRCC1.[8] In contrast, O6meG is repaired by O6meG-DNA methyltransferase (MGMT) in a one-step process removing the methyl group from the damaged base transferring it to the protein. It has previously been shown that MGMT is the main repair pathway for repair of O6meG,[9] and the cellular MGMT level has therefore great impact on the toxicity of alkylating agents.

Alkylation damage has previously been demonstrated to disturb cell cycle progression and origin firing in yeast[10] and human cells.[11] The central S-phase checkpoint kinases ATM and ATR are both involved in the alkylation damage response as deficient cells are hypersensitive to alkylating agents[12,13] and downstream targets of ATM and ATR are phosphorylated in response to MMS.[14] Although it is established that alkylations inhibit replication elongation overall,[15] it is still unclear how they directly influence replication forks in mammalian cells. Stalled replication forks are stabilised by the Chk1 kinase[16,17] and can either restart or collapse into a DNA double-strand break (DSB), which needs to be repaired by RAD51-mediated homologous recombination (HR).[18,19] Formation of collapsed replication forks following treatment with alkylating agent is supported by the fact that both MMS and MNNG induce sister chromatid exchange[5,20] and HR in both yeast[21] and mammalian cells.[22–24] However, in this case, there is evidence that the induction of HR is related to O6meG and depends on mismatch-repair-mediated DSBs produced in the second round of replication.[25–27] Thus, there is so far no evidence that HR is directly triggered at alkylation stalled replication forks.

When analyzing the effect of alkylations on *in vitro* replication using purified DNA polymerases, N-alkylations are most potent in inhibiting elongation.[28,29] O6meG efficiently blocks replication elongation *in vitro*,[30–32] but this effect is generally thought not to be the case *in vivo*, where it is bypassed and causes mispairing with thymidine (dT), inducing mutations.[33] N3meA has been predicted as a replication fork blocking lesion due to the importance of DNA polymerase contacts with N^3-purine in the minor groove.[34] The instability of N^7- and N^3-purine adducts has prevented more thorough *in vitro* studies. Both abasic sites resulting from depurination of N-alkylations, SSB repair intermediates and BER machinery present at unrepaired lesions are potential replication fork blocks.

Several pathways have been implicated in facilitating DNA replication progression through alkylated DNA, including translesion synthesis (TLS) polymerases and HR. Both DNA polymerases Pol η and Pol ζ have been suggested for TLS past O6meG.[35,36]

The effect by alkylating agents on replication fork elongation may be important for the selective killing of replicating cancer cells. Here, we investigate replication progression following alkylating damage in Chinese hamster ovary cells and find that the alkylation grade is directly proportional to the inhibition of replication. We further study the mechanism of replication inhibition and show that alkylation of DNA causes a direct block to the replication progression in contrast to slowing the replication rates. This mechanism is independent of DNA damage signalling and not influenced by caffeine inhibition of ATM and ATR. We find that the replication block is likely not owing to conversion of BER-induced SSBs into one-ended DSBs by a runoff mechanism, as there is no correlation between SSB formation and replication block. We further show that methylation of the O6 position of guanine is not responsible for the replication block.

In addition, we demonstrate that the alkylation-induced stalling of replication forks results in DNA damage, presumably DNA DSBs.

Results

Alkylation level correlates with the amount of replication inhibition

Here, we wanted to determine the grade of replication inhibition produced by alkylating agent MMS. If alkylations pose a direct block to the replication fork machinery, as each individual fork successively would encounter a DNA lesion, the density of alkylations on the template would correlate with the effect on replication fork elongation.

To determine the general effect by MMS, we first monitored cell cycle progression. AA8 cells were synchronised by a double-thymidine block prior to 15 min MMS treatment and then released into fresh media. After synchronisation with double-thymidine block, most of the cells are in early S phase. When control cells are released, they complete S phase within 4 h and finally return back to G1 to start a new cell cycle. In contrast, MMS-treated cells do not complete S phase until 9 h after release (Fig. 1a). In addition, we found that treatment with MMS results in a G2/M arrest, indicating accumulation of replication-associated DNA damage during progression through S phase with a damaged template.

There can be many explanations for delayed progression through S phase after DNA damage; thus, we next wanted to study the specific effect on replication elongation. Using the DNA fibre technique, we are able to observe single DNA fibre molecules and study individual replication forks.[37] DNA was labelled with 5-chlorodeoxyuridine (CldU) incorporation for 20 min and then labelled with 5-iododeoxyuridine (IdU) in the presence

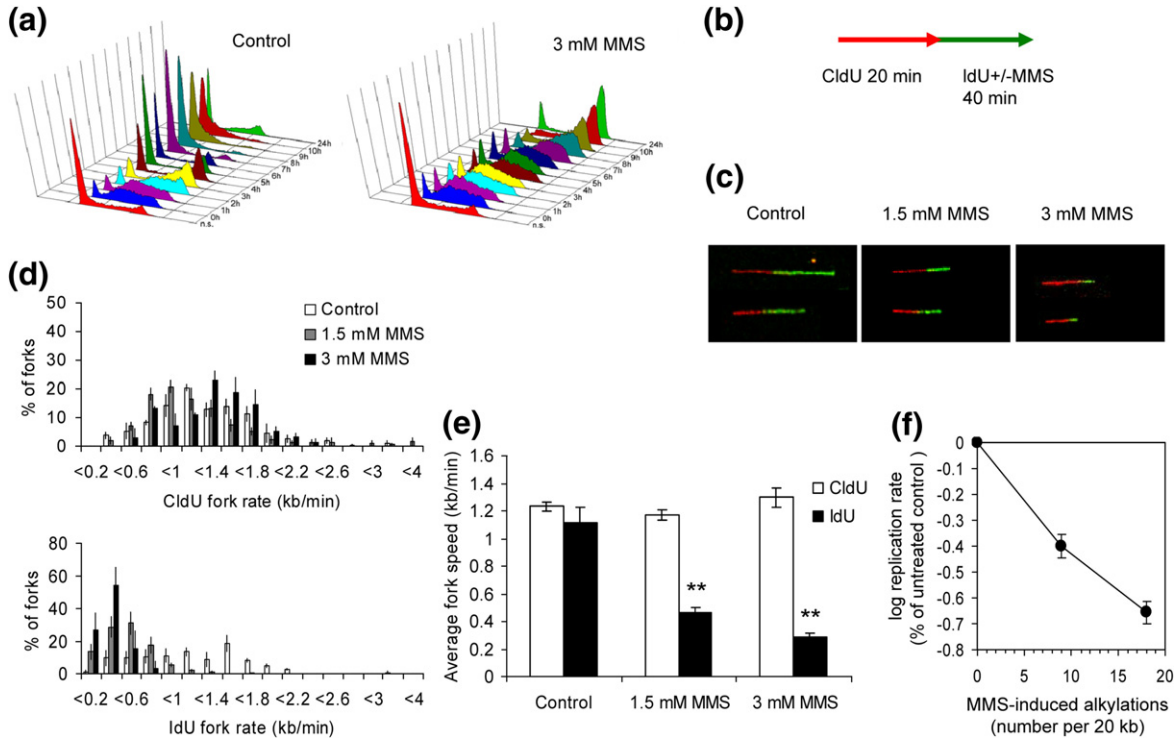

Fig. 1. MMS inhibits replication in a dose-dependent manner. (a) FACS analysis showing the effect of MMS treatment on cell cycle progression. AA8 cells were synchronised with thymidine, treated with 3 mM MMS for 15 min and released into fresh medium. Samples for FACS analysis were taken at indicated times. (b) Schematic picture of CldU/IdU labelling and MMS treatment. (c) Representative images of replication tracts from AA8 cells pulse labelled with 25 μM CldU for 20 min (red tracks) followed by 250 μM IdU for 40 min (green tracks). Treatment with either 1.5 or 3 mM MMS was given simultaneously with IdU labelling. (d) Distribution of CldU and IdU replication rates for control and MMS-treated AA8 cells. CldU showing rates before treatment and IdU showing rates during treatment. (e) Average replication rates for CldU and IdU incorporation following control and MMS treatment. (f) Reduction of replication rate plotted against number of MMS-induced alkylations on 20 kb DNA. The means and standard errors of three independent experiments are shown.

of MMS treatment for 40 min (Fig. 1b). We found that the rate of IdU incorporation was efficiently slowed in the presence of MMS. Both the dose of 1.5 and 3 mM potently inhibit replication elongation (Fig. 1c and d). Replication inhibition was found to be proportional to the amount of alkylations induced as the double dose of MMS halved the IdU replication rates comparing 1.5 and 3 mM (Fig. 1e).

The distance IdU-labelled replication forks travel in the presence of MMS is mostly shorter than the distance untreated CldU-labelled replication forks travel; that is, the red-labelled DNA track is often longer than the green-labelled one. In the CldU treatment, the fork travels about 20 kb during the 20-min labelling. A DNA alkylation needs to be present within 20 kb of DNA if MMS lesions cause a physical block to the replication fork. From the reactivity of MMS, we recalculate the number of alkylations produced on a 20-kb DNA stretch by 1.5- and 3-mM MMS treatment to 9 and 18, respectively (Table 1). We plotted the log fork rates of MMS-treated cells to the number of MMS-induced alkylations produced and find a linear relationship between the number of alkylations and reduction of fork speeds (Fig. 1f).

Alkylation of DNA cause direct replication block

Alkylations could affect replication progression in two possible ways, either by decreasing replication fork elongation speeds or by posing a direct physical block. To determine if alkylations pose a direct block to replication in contrast to slowing the replication rates, we again used the DNA fibre technique. In this case, MMS treatment was present during the first labelling with CldU. MMS and CldU were washed out at time points 15, 30 or 60 min, and IdU label was added for 20 min without MMS (Fig. 2b). If after MMS treatment replication forks were still active but progressing slowly, the CldU-labelled forks would continue to incorporate IdU. After 15 min of MMS/CldU treatment, replication forks were incorporating IdU (Fig. 2a), showing active forks. At the 30-min time point, there was still IdU incorporation but to a lesser extent (Fig. 2a). The ratio of CldU track length to IdU track length increased from 15- to 30-min MMS treatment (Fig. 2b), showing shortening of the IdU-labelled part of the fork with increasing times of MMS treatment. After 60 min of MMS/CldU treatment, no incorporation of IdU could be detected, demonstrating that replication forks were completely blocked.

Replication inhibition by alkylation is not dependent on DNA damage signalling

MMS treatment has previously been shown to activate DNA damage signalling.[12–14] Cell survival is decreased in ATM- and ATR-deficient cells,[12,13] and phosphorylation of downstream targets of ATM and ATR has been detected after MMS treatment.[14] It has also been demonstrated that S-phase progression following MMS treatment is further reduced in cells treated with ATM inhibitor.[14] However, the pronounced S-phase delay by MMS in combination with a PARP inhibitor can be reversed by addition of caffeine or expression of a dominant-negative ATR mutant.[40] Thus, there are conflicting data on the role of the DNA damage checkpoint on progression of the cell cycle.

To test the possibility that the MMS-induced replication inhibition is caused by damage signalling and not a physical block produced by alkylation lesions or repair intermediates, we preformed DNA combing in the presence of caffeine. Caffeine is a general kinase inhibitor that will inhibit both ATM and ATR at the dose of 5 mM.[41] The experiment was preformed as previously described, using CldU labelling for 20 min and then treatment with 1.5 mM MMS in the presence of IdU for 40 min. Caffeine-treated samples were pre-treated with caffeine 1 h before CldU labelling and caffeine was then present throughout the experiment (Fig. 3a). The overall CldU replication rates (in the absence of MMS) were reduced in the presence of caffeine compared to control (Fig. 3b). This was not unexpected since normal replication rates have

Table 1. Alkylation grade and replication elongation block produced following 40 min MMS and MNNG treatments

	MMS	MMS	MNNG	
Concentration (mM)	1.5	3	0.020	
DNA reactivity (μmol/g DNA and mM h)	0.90	0.90	84	[23]
Total alkylations (μmol/g DNA)	0.67	1.35	84	
No. of alkylations in the human genome	1.3×10^6	2.7×10^6	1.7×10^6	
No. of alkylation per 20 kb	9	18	11	
% alkylation on O6meG	0.31	0.31	7.0	[3,38,39]
Total O6meG alkylations (nmol/g DNA)	2.1	4.2	59	
% replication of untreated control[a]	40	22	48	
% replication reduction factor[b]	−0.036	−0.036	−0.029	

[a] Data from DNA fibre experiments in Figs. 1 and 5 (rate IdU speed in MMS/rate CldU speed control).
[b] Replication reduction factor (slope of log replication speed *versus* number of alkylations).

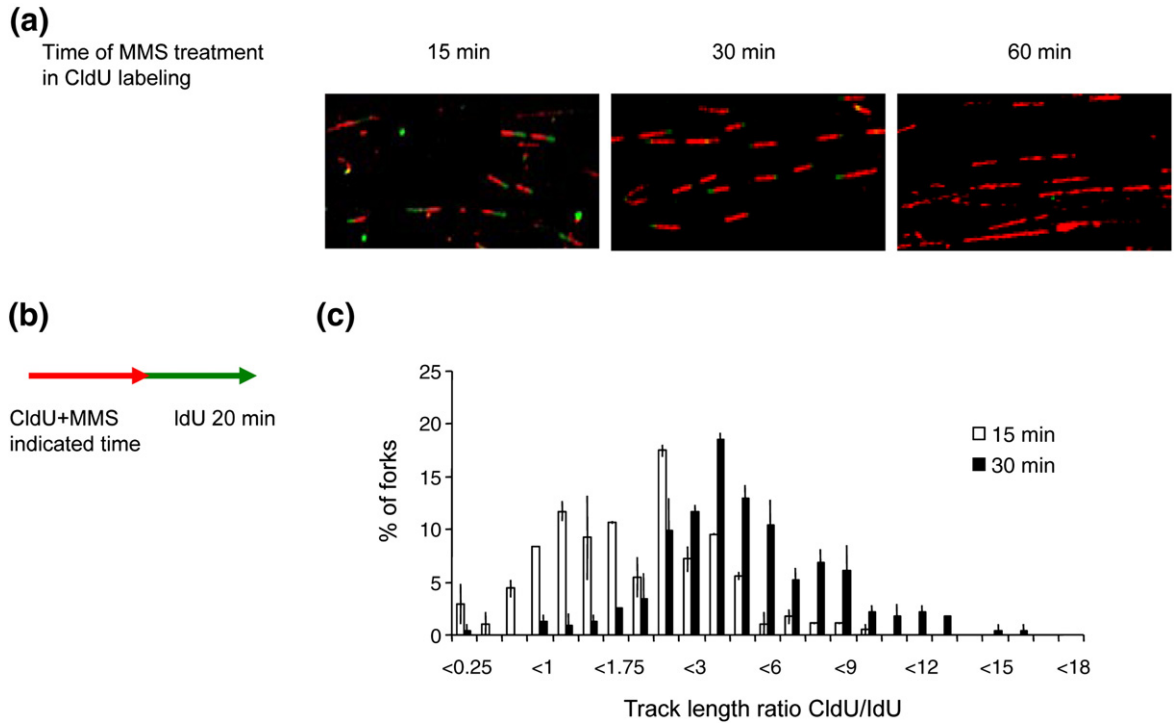

Fig. 2. MMS induces direct replication block. (a) Representative images of replication tracts from AA8 cells pulse labelled with 25 μM CldU + 1.5 mM MMS treatment for indicated times (red tracks) followed by 250 μM IdU for 20 min (green tracks). (b) Schematic picture of CldU/IdU labelling and MMS treatment. (c) Distribution of replication track length ratios for 15 and 30 min CldU + 1.5 mM MMS-treated AA8 cells. The means and standard errors of three independent experiments are shown.

been shown to be dependent on the ATR/CHK1 pathway.[42,43] Although the overall replication rates were slowed, caffeine treatment did not prevent the MMS-induced inhibition of replication. The CldU/IdU track length ratios of MMS and MMS+ caffeine-treated samples were not significantly different (Fig. 3c). Altogether, this shows that damage signalling is not involved in inhibition of replication by MMS, which further supports our finding that alkylations pose a direct block to replication.

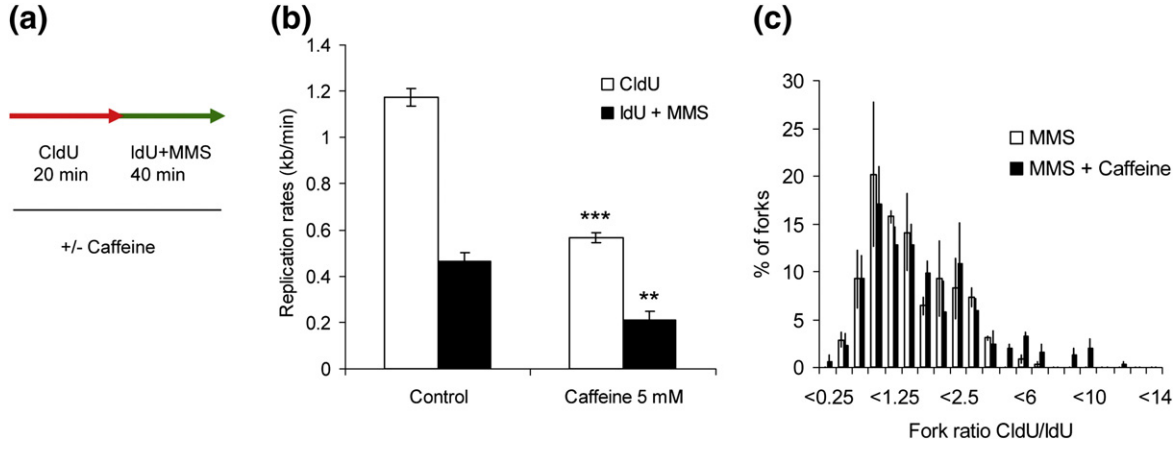

Fig. 3. MMS-induced replication slowing is not affected by caffeine. (a) Schematic picture of CldU/IdU labelling and MMS treatment. (b) Average replication rates for CldU and IdU incorporation following treatment with MMS with or without caffeine in AA8 cells. (c) Distribution of replication track length ratios for 1.5 mM MMS and 1.5 mM MMS+ caffeine-treated samples. The means and standard errors of three independent experiments are depicted.

Level of DNA SSBs does not affect block of replication progression

Because alkylations are removed by BER, the intermediates of this repair process are likely present at alkylation stalled replication forks and cells with impaired BER have more pronounced S-phase delay in response to MMS.[14] DNA SSBs encountered by the replication fork have been shown to cause replication fork collapse into DSBs triggering HR.[19,44] BER-deficient cells have spontaneously elevated frequencies of sister chromatid exchange and RAD51 foci,[45–48] and it has been suggested that SSBs formed during BER block replication by a runoff mechanism. To address this, we conducted experiments with BER-deficient cell line EM9 derived from AA8. The cell line is deficient in XRCC1 protein, resulting in a slow ligation of BER-induced SSBs.[49] Measuring the level of SSBs following 15 min of MMS treatment with the ADU technique, previously described by Johansson *et al.*,[50,51] shows that EM9 cells accumulate a high level of unligated SSBs compared to AA8 cells (Fig. 4a). To study if this elevated level of SSBs correlates with the inhibition of replication fork progression, we measured the replication fork speed in EM9 cells following MMS treatment. DNA was labelled with CldU incorporation for 20 min and then labelled with IdU in the presence of 3 mM MMS treatment for 40 min (Fig. 4c). Surprisingly, we found that EM9 cells had the same average replication fork speed as AA8 cells (Fig. 4b), demonstrating that SSB level is not influencing replication fork progression. Neither could the CldU/IdU ratio of AA8 and EM9 cells following MMS treatment be statistically separated ($p = 0.49$) (Fig. 4d).

O6meG does not influence replication bypass

For further investigation of how alkylations block replication forks, we specifically address whether the highly toxic alkylation O6meG is blocking replication elongation. We here overexpressed MGMT by transient transfection, which removes O6meG in DNA by direct reversal,[9] in AA8 cells. The AA8 Chinese hamster ovary cells have a very low endogenously expressed MGMT level, here compared to MGMT level in human RKO cells (Fig. 5a). Since the DNA fibre assay analyses replication in individual cells, it is important to confirm that all cells express the MGMT–green fluorescent protein (GFP) fusion protein following transient transfection. By fluorescence-activated cell sorting (FACS) analysis, we could detect that all cells were GFP

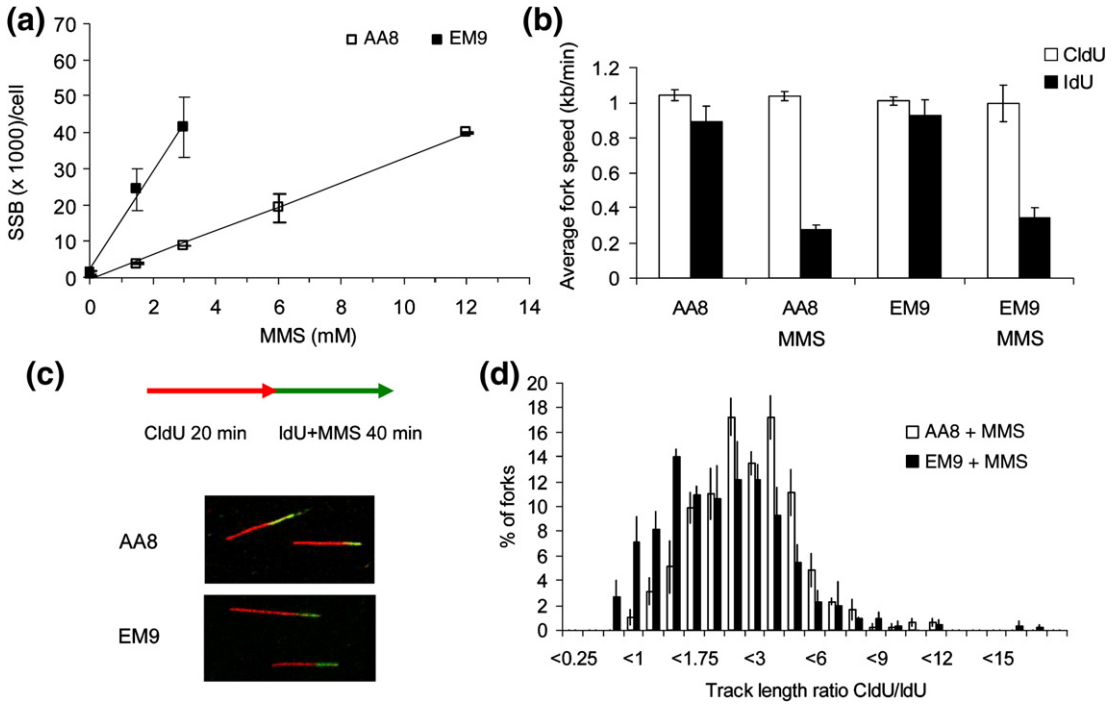

Fig. 4. Level of SSBs does not affect MMS-induced replication inhibition. (a) ADU experiment showing SSB level in AA8 cells and XRCC1-deficient EM9 cells following 15 min of MMS treatment. (b) Average replication rates for CldU and IdU incorporation following control and 3 mM MMS treatment in AA8 and EM9 cells. (c) Schematic picture of CldU/IdU labelling and MMS treatment. (d) Distribution of replication track length ratios for AA8 and EM9 cells following 3 mM MMS treatment. The means and standard errors of three independent experiments are shown.

positive (Fig. 5a). Only 0.3% of the total alkylation grade produced by MMS is O6meG, whereas MNNG has different reaction spectra and produces 7% of the total alkylations on the O6 position.[3] To test the function of the transfected MGMT construct, we performed survival and observed that MGMT–GFP expression significantly increased the survival to MNNG, but not to MMS (Fig. 5b). The difference in increased survival between MNNG- and MMS-treated cells reflects the difference in induction of O6meG by the two compounds.

We again turned to the DNA fibre technique to investigate if fork rates after 20 μM MNNG or 3 mM MMS treatment were influenced by MGMT expression. We here found that the fork rates were reduced by both MNNG and MMS regardless of the expression of MGMT–GFP (Fig. 5d), which overall suggests that O6meG does not block replication fork progression in mammalian cells. The dose of 20 μM MNNG produces a high amount of O6meG (Table 1) and has a 100% toxicity in non-MGMT-expressing AA8 cells (Fig. 5b). In contrast, the overall level of alkylations on DNA produced by 20 μM MNNG is lower than the level of alkylations produced by 3 mM MMS (Table 1), explaining why the incorporation rate of IdU is less affected by MNNG than by MMS (Fig. 5d). This is in agreement with our previous result showing that the amount of alkylations corresponds well to the replication inhibition by these compounds.

DNA damage is formed at MMS-blocked replication forks

Alkylating agents induce a potent block to DNA replication progression resulting in vulnerable stalled replication fork structures. Although SSBs are not the direct cause of the replication block, as we previously showed here, it has been demonstrated that SSBs persisting during replication can cause collapse of replication forks into DSBs.[19,52] An SSB intermediate is formed during the repair of N-alkylations,[8] which, if persisting potentially, can be converted to a collapsed replication fork. Thus, there is a possibility that DSBs are formed at forks encountering alkylation damage. To test this, we labelled newly replicating DNA with BrdU 15 min prior to MMS treatment and then waited 4 h to allow replication fork block. We then stained SPD8 cells for phosphorylation on H2AX (γH2AX), which is as

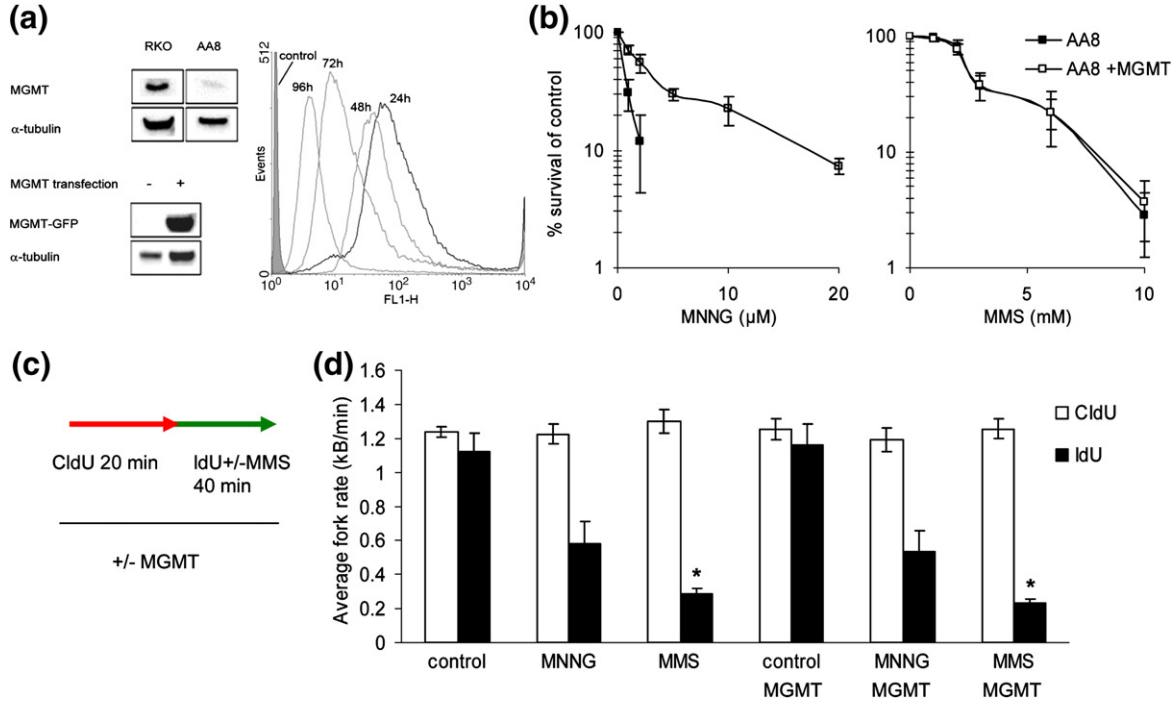

Fig. 5. Replication rates are not affected by O6meG. (a) WB showing endogenous levels of MGMT expression in AA8 cells compared to RKO cells and WB showing GFP expression in AA8 cells with or without transfection with MGMT–GFP construct. FACS analysis showing GFP signal in AA8 cells over time after transfection with MGMT–GFP. (b) Survival of AA8 cells following treatment with MNNG and MMS, with or without transient transfection with MGMT–GFP construct. The means and standard deviations of three independent experiments are shown. (c) Schematic picture of CldU/IdU labelling and MMS treatment. (d) Average replication rates for CldU and IdU incorporation following treatment with 20 μM MNNG or 3 mM MMS, with or without MGMT–GFP transient transfection. The means and standard errors of three independent experiments are shown.

a marker for DNA damage. Here, we report that BrdU-labelled sites of replication co-localise with γH2AX foci after MMS treatments (Fig. 6a).

We found an overall higher amount of γH2AX produced 4 h after MMS treatment than after MNNG treatments (Fig. 6c), even though there is a 14 times higher O6meG alkylation grade with MNNG than after the MMS treatment used here (Table 1). This suggests that the γH2AX foci are not caused by O6meG but are more likely being correlated to replication arrest, which is also supported by the co-localisation with newly replicated areas (Fig. 6a). It is well established that γH2AX foci form at sites of DSBs;[53] however, γH2AX foci also form after UV treatment in the absence of DSBs[54] as well as at hydroxyurea stalled replication forks that can easily restart and are not associated with DSBs.[18] Formation of DSBs following MMS treatment cannot be detected with pulse-field gel electrophoresis (PFGE),[23] possibly because of the low sensitivity of the method. To further investigate the damage pattern after MMS-induced replication arrest, we stained MMS-treated SPD8 cells for 53BP1. 53BP1, a p53 interacting protein[55] also used as a DSB marker, has been shown to co-localise with γH2AX after γ-radiation but not to form foci in response to UV.[56] We discovered that MMS treatment results in a strong 53BP1 response where the 53BP1 foci to a high extent co-localise with γH2AX foci 4 h after treatment (Fig. 6b).

In conclusion, we show that MMS induces large amounts of γH2AX foci co-localising with newly replicated areas and 53BP1 foci, indicating that DSBs are formed at alkylation stalled replication forks.

Discussion

Although it has previously been demonstrated that MMS perturbs replication fork progression,[15] the underlying reason for this effect has not been studied. Here, we argue that the replication fork block by MMS is explained by a physical block to the replication machinery. Although *in vitro* and structural data suggested that methylated purines may form a physical block to replication,[29,34] the situation in mammalian cells may be different due to the presence of several highly effective TLS polymerases. Here, we report a linear dose–response relationship between increasing MMS dose and reduction of replication fork elongation (Fig. 1f), which is what would be expected if replication forks are blocked by alkylated DNA lesions. When recalculating the number of total alkylations required for reduction of replication rates, we find that the replication fork is significantly slowed even by a few alkylations (Fig. 1f; Table 1). This suggests that a common alkylation induced by MMS treatment is responsible for replication fork block, that is, N7meG or N3meA.[4] Previously, it has been shown *in vitro* that N3meA is a replication-stalling lesion.[29] In the same study, Larson *et al.* also showed that apurinic sites resulting from depurinations of N-alkylations, such as N7meG or N3meA, blocked replication elongation.

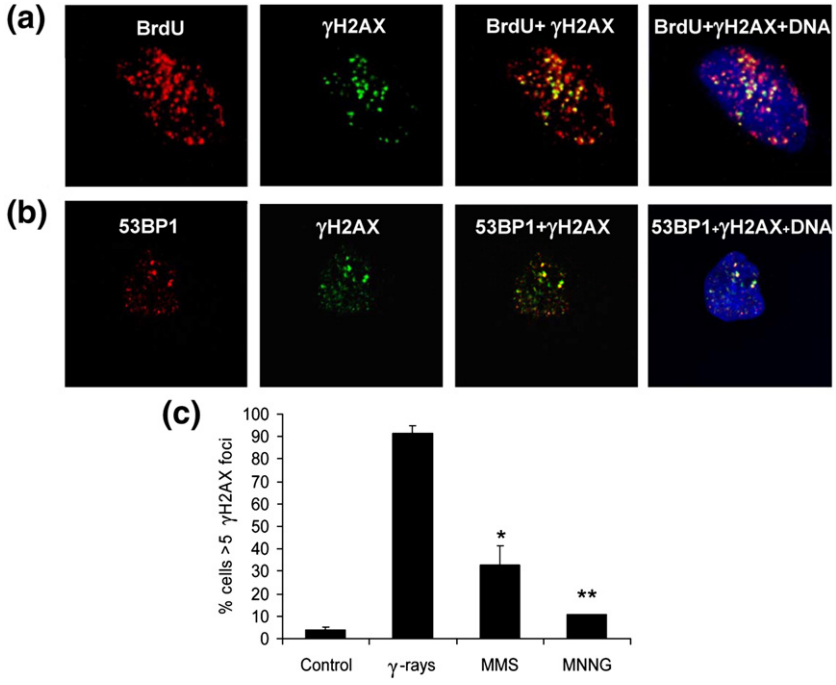

Fig. 6. MMS triggers formation of γH2AX and 53BP1 foci at replication sites. (a) γH2AX foci co-localise with replication sites marked by 15 min BrdU labelling of newly replicated DNA prior to 3 mM MMS treatment for 30 min. Picture showing SPD8 cells at 4 h post-treatment. (b) γH2AX foci co-localise with 53BP1 foci in SPD8 cells 4 h following 3 mM MMS treatment. (c) Percentage of cells displaying γH2AX foci 4 h after treatment with 10 Gy of γ-rays, 3 mM MMS or 10 μM MNNG. The mean percentages of cells containing γH2AX foci and standard deviations from three independent experiments are depicted.

It has been suggested that SSBs formed during BER will block the replication fork and lead to replication fork collapse triggering HR.[57,58] However, in this study, we found no support for this theory. The EM9 cell line deficient in the SSB repair step of BER exhibits elevated levels of SSBs after MMS treatment as expected but does not show increased replication block. If the replication block is explained by a runoff mechanism of a persisting SSB intermediate during BER, it would be anticipated that more SSB intermediates would more profoundly arrest replication fork speed.

Activation of DNA damage checkpoints have been demonstrated in the alkylation-induced damage response.[12] The S-phase delay after MMS treatment in yeast[59] is the result of reduced origin firing and checkpoint-independent reduction of replication rates.[10] Here, we confirm that the checkpoint independence also applies to mammalian cells where inhibition of checkpoint kinases ATM and ATR by caffeine does not influence the MMS-induced replication inhibition. ATR and PARP-1 are both activated at stalled replication forks[13,37,60] and both protect cells from cytotoxic effects caused by MMS.[40,61,62] The pronounced S-phase delay previously shown in BER-deficient cells requires damage signalling[14] and could be a result secondary replication-associated damage. We suggest that the DNA damage signalling is not involved in the formation of MMS-induced replication block, but rather has a role in the maintenance of the stability of the stalled fork, repair, replication restart and activation of cell death pathways.

O6meG is mutagenic by its base paring with T during replication[33] and has never been shown to affect cell cycle progression during the first S phase, suggesting that the O6meG lesion is efficiently bypassed in cells. However, *in vitro* data suggest that O6meG efficiently blocks replication elongation[30–32] and that TLS polymerases such as Pol η or Pol ζ are needed to bypass O6meG.[35,36] Here, we show that MMS and MNNG block replication fork elongation. Although MNNG produced 14 times more O6meG lesions than MMS by the doses used here (Table 1), we find that MMS treatment blocks replication elongation more efficiently. This suggests that alkylations other than O6meG are responsible for the replication arrest. Further evidence that O6meG does not block replication elongation *in vivo* is that expression of MGMT–GFP has no effect on replication elongation, despite increasing the tolerance to MNNG treatments about 10-fold (Fig. 3). These data suggest that bypass of O6meG lesions is highly efficient and that this lesion does not constitute a block for replication fork progression.

It is an accepted theory that stalling of replication progression could result in replication forks collapsing into DSBs.[63,64] In mammalian cells, replication-associated DSBs have been demonstrated after stalling of replication progression by depletion of the nucleotide pool with hydroxurea.[65] Here, we also investigated the consequences of replication forks being stalled by alkylation damage. We found that γH2AX foci form 4 h following treatment at sites where replication forks were situated at the time of treatment. γH2AX is a marker for DNA damage, but it has been disputed if this damage is limited to DSBs as foci are formed after UV damage not resulting in DSBs.[54] Interestingly, we here observed that the γH2AX foci formed following MMS treatment also co-localise with 53BP1. 53BP1 has been reported to form foci in response to γ-radiation but not in response to UV[56] and is generally believed to be a more specific marker for DSBs. We suggest that MMS stalled replication forks collapse into replication-associated DSBs. γH2AX and 53BP1 foci increased progressively from the time of treatment up to the last 4-h time point (data not shown), supporting the theory that replication fork collapse is not immediate. We have not been able to detect DSB induction by MMS treatments using PFGE[23] (data not shown). The likely reason is that MMS-induced DSBs are too few to be visualised by PFGE.

In summary, the data presented here demonstrate that the altered replication fork progression following alkylation damage is a result of a direct physical replication block, which is associated with formation of DNA damage. The lesion responsible for the block is likely N7meG or N3meA and not O6meG. We could not find evidence that BER-induced SSBs are causing replication forks to stall but formation of a replication block by BER factors cannot be excluded. Inhibition of DNA damage signalling does not affect alkylation-induced replication block, which supports a model where checkpoint cascades are triggered for stabilisation of blocked replication forks.

Materials and Methods

Cell culture

All cell lines were cultured in Dulbecco's modified Eagle's medium, with the addition of 9% fetal calf serum and penicillin–streptomycin (90 U/ml), at 37 °C and 5% CO_2 atmosphere.

Transfection with MGMT–GFP construct

MGMT transfectants were generated by transfection of AA8 cells with the mammalian expression vector pEGFP-N2 harbouring the MGMT–EGFP fusion gene described elsewhere.[66] Transfection was performed with the Lipofectamine2000 kit for 6 h at 37 °C in medium without fetal calf serum and antibiotics. Transfection

efficiency was controlled by flow cytometry and Western blot.

Treatments

One-hundred-millimolar stock solution of MNNG and 11.8 M stock solution of MMS were prepared by dissolving these agents in dimethyl sulfoxide. The MNNG stock solution was aliquoted and both agents were stored at 4 °C until used. Hanks balanced salt solution (HBSS) (GIBCO) or medium (Dulbecco's modified Eagle's medium) was used for dilution of MMS and MNNG directly before treatment. Caffeine was dissolved directly in media. All treatments were preformed in 37 °C and 5% CO_2 atmosphere. Cells were rinsed 3 times with HBSS following treatment if not harvested directly.

Toxicity assay

Five hundred AA8 cells were plated per cell culture dish (area of 10 cm^2/well) 24 h prior to treatment with MNNG or MMS. Following treatments, plates were rinsed 3 times with HBSS and fresh medium was added. After 7 to 10 days, the plates were harvested and colonies were fixed and stained using methylene blue in methanol (4 g/L). Colonies containing more than 50 cells were counted.

Flow cytometry

AA8 cells were synchronised to G1/S boundary by double-thymidine block. Cells were sequentially incubated with medium containing 2 mM thymidine for 12 h, normal medium for 6 h, and 2 mM thymidine for 12 h. Finally, synchronised cells were treated and then released in medium. At the indicated time points, cells were washed once with phosphate-buffered saline (PBS) and then fixed with 70% (v/v) and incubated for at least 2 h. Before analysis, cells were incubated in 500 μl PBS containing 2 μl propidium iodide and 40 μl RNase A for 30 min at room temperature. Cell cycle profiles were acquired on a FACSCalibur instrument (Becton Dickinson) using CellQuest Pro software.

Western blot analysis

Cells were washed with PBS twice on ice before adding protein lysis buffer (1× protease inhibitor cocktail, Roche Basel, Switzerland, 1.5 mM ethylenediaminetetraacetic acid, 1 mM DTT, 10% glycerol and 25 mM Hepes, pH 7.6). The protein concentration was determined using the Bradford assay (Hercules, CA). Total protein (20 μg) was resolved by 7–12% SDS-PAGE for subsequent Western blot analysis using antibodies against the following proteins diluted in PBS as indicated: α-tubulin (1:10,000) and MGMT (1:1000). The gel was transferred to a nitrocellulose membrane and immunoblotted with primary antibody. Anti-mouse or rabbit IgG conjugated to horseradish peroxidase was used as the secondary antibody for detection using an ECL Western blot detection system.

Immunofluorescence

SPD8 cells (5×10^4) were plated onto coverslips and treated with 3 mM MMS or 10 μM MNNG for 0.5 h or γ-irradiated (^{137}Cs, 0.56 Gy/min). Following treatment, the medium was removed and the coverslips were rinsed once in PBS (37 °C) and fixed in 3% paraformaldehyde in PBS-T (PBS containing 0.1% Triton X-100 and 0.15% bovine serum albumin) for 20 min. The coverslips were rinsed twice in PBS-T prior to incubation with a mouse monoclonal anti-phospho-Histone H2AX (Ser139) (Upstate Biotechnology, 1:1000) for 16 h in 4 °C and rabbit anti-53BP1 (Bethyl Laboratories Inc., 1:500) for 1 h at room temperature or rabbit anti-53BP1(Bethyl Laboratories Inc., 1:500) for 1 h at room temperature. The coverslips were rinsed 4×15 min in PBS-T followed by 1 h incubation at room temperature with a Cy-3-conjugated goat anti-mouse IgG antibody (Zymed) at a concentration of 1:500 and then rinsed 4×15 min in PBS-T. Antibodies were diluted in PBS containing 3% bovine serum albumin. DNA was stained with 1 μg/ml To Pro (Molecular Probes). Coverslips were mounted with SlowFade Antifade Kit (Molecular Probes). Images were obtained with a Zeiss LSM 510 inverted confocal microscope using planapochromat 63×/NA 1.4 oil immersion objective and excitation wavelengths 546 and 630 nm. Through focus, maximum projection images were acquired from optical sections 0.50 μm apart and with a section thickness of 1.0 μm. The frequencies of cells containing γH2AX foci were determined by counting at least 300 nuclei in each slide in each experiment. Nuclei containing more than 5 foci were classified as γH2AX positive.

DNA fibre technique

AA8 cells were plated 24 h prior to treatment. For measuring of replication rates, labelling with 25 μM CldU (Sigma, C6891-100MG) was preformed in media for 20 min. CldU media were then replaced with media containing 250 μM IdU (Sigma I7125-5G) with or without treatment with MMS or MNNG. IdU labelling and treatment were then aborted after 40 min. For measuring of replication block, cells were labelled with CldU + MMS for indicated time points. Cells were then rinsed with HBSS 3 times and IdU labelling was added for 20 min. For both experiments, cells were scraped and harvested in cold PBS. Cells were spun down, counted, and diluted to a concentration of 5×10^5 cells/ml. A drop of cell suspension together with spreading buffer (200 mM Tris–HCl, pH 7.4, 50 mM ethylenediaminetetraacetic acid and 0.5% SDS) was put on a microscope slide and incubated for a few minutes where the lysing of cells took place. The slide was then tilted so that DNA fibres could spread over the slide. Slides were air dried and the fibres were fixed on the slides with methanol/acidic acid (3:1). Staining of fibres was done with monoclonal rat anti BrdU [Clone BU1/75 (ICR1) (Oxford Biotechnologies)] for CldU and monoclonal mouse anti BrdU {(Clone B44) [Becton Dickinson, 347580 (7580)]} for IdU. Secondary antibodies were goat anti-rat AlexaFluor 555 and goat anti-mouse AlexaFluor 488. DNA fibres were studied in confocal microscope. The lengths of CldU and IdU tracks were measured using the ImageJ software and micrometer values were converted into kilobase pairs using the

conversion factor 1 μm = 2.59 kb. At least 100 forks were analyzed for every condition.

Acknowledgements

We wish to thank Drs Larry Thompson and Lene Rasmussen for providing materials and the Swedish Cancer Society, the Swedish Children's Cancer Foundation, the Swedish Research Council, the Swedish Pain Relief Foundation and the Medical Research Council for supporting this work financially.

Conflict of Interest. The authors declare no conflict of interest.

References

1. Helleday, T., Petermann, E., Lundin, C., Hodgson, B. & Sharma, R. A. (2008). DNA repair pathways as targets for cancer therapy. *Nat. Rev., Cancer*, **8**, 193–204.
2. Pullman, A. & Pullman, B. (1981). Molecular electrostatic potential of the nucleic acids. *Q. Rev. Biophys.* **14**, 289–380.
3. Roberts, J. J., Pascoe, J. M., Plant, J. E., Sturrock, J. E. & Crathorn, A. R. (1971). Quantitative aspects of the repair of alkylated DNA in cultured mammalian cells. I. The effect on HeLa and Chinese hamster cell survival of alkylation of cellular macromolecules. *Chem. Biol. Interact.* **3**, 29–47.
4. Wyatt, M. D. & Pittman, D. L. (2006). Methylating agents and DNA repair responses: methylated bases and sources of strand breaks. *Chem. Res. Toxicol.* **19**, 1580–1594.
5. Kaina, B., Fritz, G., Mitra, S. & Coquerelle, T. (1991). Transfection and expression of human O^6-methylguanine-DNA methyltransferase (MGMT) cDNA in Chinese hamster cells: the role of MGMT in protection against the genotoxic effects of alkylating agents. *Carcinogenesis*, **12**, 1857–1867.
6. Cai, Y., Wu, M. H., Xu-Welliver, M., Pegg, A. E., Ludeman, S. M. & Dolan, M. E. (2000). Effect of O^6-benzylguanine on alkylating agent-induced toxicity and mutagenicity in Chinese hamster ovary cells expressing wild-type and mutant O^6-alkylguanine-DNA alkyltransferases. *Cancer Res.* **60**, 5464–5469.
7. Karran, P. & Marinus, M. G. (1982). Mismatch correction at O^6-methylguanine residues in *E. coli* DNA. *Nature*, **296**, 868–869.
8. Wilson, S. H. & Kunkel, T. A. (2000). Passing the baton in base excision repair. *Nat. Struct. Biol.* **7**, 176–178.
9. Lindahl, T., Demple, B. & Robins, P. (1982). Suicide inactivation of the E. coli O^6-methylguanine-DNA methyltransferase. *EMBO J.* **1**, 1359–1363.
10. Tercero, J. A. & Diffley, J. F. (2001). Regulation of DNA replication fork progression through damaged DNA by the Mec1/Rad53 checkpoint. *Nature*, **412**, 553–557.
11. Painter, R. B. (1977). Inhibition of initiation of HeLa cell replicons by methyl methanesulfonate. *Mutat. Res.* **42**, 299–303.
12. Barfknecht, T. R. & Little, J. B. (1982). Hypersensitivity of ataxia telangiectasia skin fibroblasts to DNA alkylating agents. *Mutat. Res.* **94**, 369–382.
13. Cliby, W. A., Roberts, C. J., Cimprich, K. A., Stringer, C. M., Lamb, J. R., Schreiber, S. L. & Friend, S. H. (1998). Overexpression of a kinase-inactive ATR protein causes sensitivity to DNA-damaging agents and defects in cell cycle checkpoints. *EMBO J.* **17**, 159–169.
14. Brem, R., Fernet, M., Chapot, B. & Hall, J. (2008). The methyl methanesulfonate induced S-phase delay in XRCC1-deficient cells requires ATM and ATR. *DNA Repair (Amst.)*, **7**, 849–857.
15. Merrick, C. J., Jackson, D. & Diffley, J. F. (2004). Visualization of altered replication dynamics after DNA damage in human cells. *J. Biol. Chem.* **279**, 20067–20075.
16. Syljuasen, R. G., Sorensen, C. S., Hansen, L. T., Fugger, K., Lundin, C., Johansson, F. *et al.* (2005). Inhibition of human Chk1 causes increased initiation of DNA replication, phosphorylation of ATR targets, and DNA breakage. *Mol. Cell. Biol.* **25**, 3553–3562.
17. Sorensen, C. S., Hansen, L. T., Dziegielewski, J., Syljuasen, R. G., Lundin, C., Bartek, J. & Helleday, T. (2005). The cell-cycle checkpoint kinase Chk1 is required for mammalian homologous recombination repair. *Nat. Cell Biol.* **7**, 195–201.
18. Petermann, E., Orta, M. L., Issaeva, N., Schultz, N. & Helleday, T. (2010). Hydroxyurea-stalled replication forks become progressively inactivated and require two different RAD51-mediated pathways for restart and repair. *Mol. Cell*, **37**, 492–502.
19. Arnaudeau, C., Lundin, C. & Helleday, T. (2001). DNA double-strand breaks associated with replication forks are predominantly repaired by homologous recombination involving an exchange mechanism in mammalian cells. *J. Mol. Biol.* **307**, 1235–1245.
20. Rasouli-Nia, A., Sibghat, U., Mirzayans, R., Paterson, M. C. & Day, R. S., 3rd (1994). On the quantitative relationship between O^6-methylguanine residues in genomic DNA and production of sister-chromatid exchanges, mutations and lethal events in a Mer- human tumor cell line. *Mutat. Res.* **314**, 99–113.
21. Hendricks, C. A., Razlog, M., Matsuguchi, T., Goyal, A., Brock, A. L. & Engelward, B. P. (2002). The *S. cerevisiae* Mag1 3-methyladenine DNA glycosylase modulates susceptibility to homologous recombination. *DNA Repair (Amst.)*, **1**, 645–659.
22. Zhang, H., Tsujimura, T., Bhattacharyya, N. P., Maher, V. M. & McCormick, J. J. (1996). O^6-Methylguanine induces intrachromosomal homologous recombination in human cells. *Carcinogenesis*, **17**, 2229–2235.
23. Lundin, C., North, M., Erixon, K., Walters, K., Jenssen, D., Goldman, A. S. & Helleday, T. (2005). Methyl methanesulfonate (MMS) produces heat-labile DNA damage but no detectable in vivo DNA double-strand breaks. *Nucleic Acids Res.* **33**, 3799–3811.
24. Helleday, T., Arnaudeau, C. & Jenssen, D. (1998). Effects of carcinogenic agents upon different mechanisms for intragenic recombination in mammalian cells. *Carcinogenesis*, **19**, 973–978.

25. Jiricny, J. (2006). The multifaceted mismatch-repair system. *Nat. Rev., Mol. Cell Biol.* **7**, 335–346.
26. Cejka, P., Mojas, N., Gillet, L., Schar, P. & Jiricny, J. (2005). Homologous recombination rescues mismatch-repair-dependent cytotoxicity of S(N)1-type methylating agents in *S. cerevisiae*. *Curr. Biol.* **15**, 1395–1400.
27. Zhang, H., Marra, G., Jiricny, J., Maher, V. M. & McCormick, J. J. (2000). Mismatch repair is required for O(6)-methylguanine-induced homologous recombination in human fibroblasts. *Carcinogenesis*, **21**, 1639–1646.
28. O'Connor, T. R., Boiteux, S. & Laval, J. (1988). Ring-opened 7-methylguanine residues in DNA are a block to in vitro DNA synthesis. *Nucleic Acids Res.* **16**, 5879–5894.
29. Larson, K., Sahm, J., Shenkar, R. & Strauss, B. (1985). Methylation-induced blocks to in vitro DNA replication. *Mutat. Res.* **150**, 77–84.
30. Voigt, J. M. & Topal, M. D. (1995). O^6-Methylguanine-induced replication blocks. *Carcinogenesis*, **16**, 1775–1782.
31. Ceccotti, S., Dogliotti, E., Gannon, J., Karran, P. & Bignami, M. (1993). O^6-Methylguanine in DNA inhibits replication in vitro by human cell extracts. *Biochemistry*, **32**, 13664–13672.
32. Ceccotti, S., MacPherson, P., Karran, P. & Bignami, M. (1994). O^6-Methylguanine in DNA inhibits DNA replication and stimulates DNA repair synthesis in vitro. *Ann. N. Y. Acad. Sci.* **726**, 340–342.
33. Eadie, J. S., Conrad, M., Toorchen, D. & Topal, M. D. (1984). Mechanism of mutagenesis by O^6-methylguanine. *Nature*, **308**, 201–203.
34. Doublie, S., Tabor, S., Long, A. M., Richardson, C. C. & Ellenberger, T. (1998). Crystal structure of a bacteriophage T7 DNA replication complex at 2.2 Å resolution. *Nature*, **391**, 251–258.
35. Haracska, L., Prakash, S. & Prakash, L. (2000). Replication past O(6)-methylguanine by yeast and human DNA polymerase eta. *Mol. Cell. Biol.* **20**, 8001–8007.
36. Haracska, L., Prakash, S. & Prakash, L. (2003). Yeast DNA polymerase zeta is an efficient extender of primer ends opposite from 7,8-dihydro-8-oxoguanine and O^6-methylguanine. *Mol. Cell. Biol.* **23**, 1453–1459.
37. Bryant, H. E., Petermann, E., Schultz, N., Jemth, A. S., Loseva, O., Issaeva, N. *et al.* (2009). PARP is activated at stalled forks to mediate Mre11-dependent replication restart and recombination. *EMBO J.* **28**, 2601–2615.
38. Lawley, P. D. & Thatcher, C. J. (1970). Methylation of deoxyribonucleic acid in cultured mammalian cells by *N*-methyl-*N*′-nitro-*N*-nitrosoguanidine. The influence of cellular thiol concentrations on the extent of methylation and the 6-oxygen atom of guanine as a site of methylation. *Biochem. J.* **116**, 693–707.
39. Lawley, P. D. & Shah, S. A. (1972). Reaction of alkylating mutagens and carcinogens with nucleic acids: detection and estimation of a small extent of methylation at O-6 of guanine in DNA by methyl methanesulphonate in vitro. *Chem. Biol. Interact.* **5**, 286–288.
40. Horton, J. K., Stefanick, D. F., Kedar, P. S. & Wilson, S. H. (2007). ATR signaling mediates an S-phase checkpoint after inhibition of poly(ADP-ribose) polymerase activity. *DNA Repair (Amst.)*, **6**, 742–750.
41. Sarkaria, J. N., Busby, E. C., Tibbetts, R. S., Roos, P., Taya, Y., Karnitz, L. M. & Abraham, R. T. (1999). Inhibition of ATM and ATR kinase activities by the radiosensitizing agent, caffeine. *Cancer Res.* **59**, 4375–4382.
42. Petermann, E. & Caldecott, K. W. (2006). Evidence that the ATR/Chk1 pathway maintains normal replication fork progression during unperturbed S phase. *Cell Cycle*, **5**, 2203–2209.
43. Maya-Mendoza, A., Petermann, E., Gillespie, D. A., Caldecott, K. W. & Jackson, D. A. (2007). Chk1 regulates the density of active replication origins during the vertebrate S phase. *EMBO J.* **26**, 2719–2731.
44. Haber, J. E. (2000). Lucky breaks: analysis of recombination in *Saccharomyces*. *Mutat. Res.* **451**, 53–69.
45. Thompson, L. H., Brookman, K. W., Jones, N. J., Allen, S. A. & Carrano, A. V. (1990). Molecular cloning of the human XRCC1 gene, which corrects defective DNA strand break repair and sister chromatid exchange. *Mol. Cell. Biol.* **10**, 6160–6171.
46. Zdzienicka, M. Z., van der Schans, G. P., Natarajan, A. T., Thompson, L. H., Neuteboom, I. & Simons, J. W. (1992). A Chinese hamster ovary cell mutant (EM-C11) with sensitivity to simple alkylating agents and a very high level of sister chromatid exchanges. *Mutagenesis*, **7**, 265–269.
47. Pinero, J. & Cortes, F. (1993). Abnormally high incidence of SCE in three successive cell cycles in the CHO mutant EM9 as detected by a three-way immunoperoxidase differential staining. *Mutat. Res.* **292**, 205–211.
48. Schultz, N., Lopez, E., Saleh-Gohari, N. & Helleday, T. (2003). Poly(ADP-ribose) polymerase (PARP-1) has a controlling role in homologous recombination. *Nucleic Acids Res.* **31**, 4959–4964.
49. Thompson, L. H., Brookman, K. W., Dillehay, L. E., Carrano, A. V., Mazrimas, J. A., Mooney, C. L. & Minkler, J. L. (1982). A CHO-cell strain having hypersensitivity to mutagens, a defect in DNA strand-break repair, and an extraordinary baseline frequency of sister-chromatid exchange. *Mutat. Res.* **95**, 427–440.
50. Johansson, F., Lundell, T., Rydberg, P., Erixon, K. & Jenssen, D. (2005). Mutagenicity and DNA repair of glycidamide-induced adducts in mammalian cells. *Mutat. Res.* **580**, 81–89.
51. Erixon, K. & Ahnstrom, G. (1979). Single-strand breaks in DNA during repair of UV-induced damage in normal human and xeroderma pigmentosum cells as determined by alkaline DNA unwinding and hydroxylapatite chromatography: effects of hydroxyurea, 5-fluorodeoxyuridine and 1-beta-D-arabinofuranosylcytosine on the kinetics of repair. *Mutat. Res.* **59**, 257–271.
52. Strumberg, D., Pilon, A. A., Smith, M., Hickey, R., Malkas, L. & Pommier, Y. (2000). Conversion of topoisomerase I cleavage complexes on the leading strand of ribosomal DNA into 5′-phosphorylated DNA double-strand breaks by replication runoff. *Mol. Cell. Biol.* **20**, 3977–3987.
53. Stucki, M., Clapperton, J. A., Mohammad, D., Yaffe, M. B., Smerdon, S. J. & Jackson, S. P. (2005). MDC1

directly binds phosphorylated histone H2AX to regulate cellular responses to DNA double-strand breaks. *Cell*, **123**, 1213–1226.
54. Marti, T. M., Hefner, E., Feeney, L., Natale, V. & Cleaver, J. E. (2006). H2AX phosphorylation within the G1 phase after UV irradiation depends on nucleotide excision repair and not DNA double-strand breaks. *Proc. Natl Acad. Sci. USA*, **103**, 9891–9896.
55. Iwabuchi, K., Bartel, P. L., Li, B., Marraccino, R. & Fields, S. (1994). Two cellular proteins that bind to wild-type but not mutant p53. *Proc. Natl Acad. Sci. USA*, **91**, 6098–6102.
56. Schultz, L. B., Chehab, N. H., Malikzay, A. & Halazonetis, T. D. (2000). p53 binding protein 1 (53BP1) is an early participant in the cellular response to DNA double-strand breaks. *J. Cell Biol.* **151**, 1381–1390.
57. Bryant, H. E., Schultz, N., Thomas, H. D., Parker, K. M., Flower, D., Lopez, E. *et al.* (2005). Specific killing of BRCA2-deficient tumours with inhibitors of poly(ADP-ribose)polymerase. *Nature*, **434**, 913–917.
58. Caldecott, K. W. (2007). Mammalian single-strand break repair: mechanisms and links with chromatin. *DNA Repair (Amst.)*, **6**, 443–453.
59. Paulovich, A. G. & Hartwell, L. H. (1995). A checkpoint regulates the rate of progression through S phase in *S. cerevisiae* in response to DNA damage. *Cell*, **82**, 841–847.
60. Zou, L. & Elledge, S. J. (2003). Sensing DNA damage through ATRIP recognition of RPA–ssDNA complexes. *Science*, **300**, 1542–1548.
61. Kedar, P. S., Stefanick, D. F., Horton, J. K. & Wilson, S. H. (2008). Interaction between PARP-1 and ATR in mouse fibroblasts is blocked by PARP inhibition. *DNA Repair (Amst.)*, **7**, 1787–1798.
62. Horton, J. K., Stefanick, D. F., Naron, J. M., Kedar, P. S. & Wilson, S. H. (2005). Poly(ADP-ribose) polymerase activity prevents signaling pathways for cell cycle arrest after DNA methylating agent exposure. *J. Biol. Chem.* **280**, 15773–15785.
63. Budzowska, M. & Kanaar, R. (2009). Mechanisms of dealing with DNA damage-induced replication problems. *Cell Biochem. Biophys.* **53**, 17–31.
64. Helleday, T., Lo, J., van Gent, D. C. & Engelward, B. P. (2007). DNA double-strand break repair: from mechanistic understanding to cancer treatment. *DNA Repair (Amst.)*, **6**, 923–935.
65. Lundin, C., Erixon, K., Arnaudeau, C., Schultz, N., Jenssen, D., Meuth, M. & Helleday, T. (2002). Different roles for nonhomologous end joining and homologous recombination following replication arrest in mammalian cells. *Mol. Cell. Biol.* **22**, 5869–5878.
66. Rasmussen, A. K. & Rasmussen, L. J. (2005). Targeting of O^6-MeG DNA methyltransferase (MGMT) to mitochondria protects against alkylation induced cell death. *Mitochondrion*, **5**, 411–417.